# NUMERICAL PORE-NETWORK FUSION TO PREDICT CAPILLARY PRESSURE AND RELATIVE PERMEABILITY IN CARBONATES

Sven Roth[1], Danyong Li[1], Hu Dong[1], Martin J. Blunt[1,2]
[1]iRock Technologies, Oriental Media Center, No. 4 Guanghua Rd., Beijing, China
[2]Department of Earth Science and Engineering, Imperial College, London SW7 2AZ, UK

*This paper was prepared for presentation at the International Symposium of the Society of Core Analysts held in Aberdeen, Scotland, UK, 27-30 August, 2012*

## ABSTRACT

In recent years, digital rock physics has gained increasing attention in the core analysis community. Since petrophysical properties are calculated on 3D (computer) rock models, digital rock analysis requires representative replicas of the original rock sample – at all scales. Using advanced imaging technology rock samples can be imaged from the core scale down to nanometer scale, revealing the complex pore structures of different rock facies. However, it is in the nature of any imaging technology that there is a trade-off between image resolution and captured volume. It is not currently possible to combine large-scale rock features (centimeter to millimeter) with sub-micron information into one single 3D model. This is a particular problem in vuggy carbonates. In this study a multi-scale approach is presented that numerically incorporates pore-networks from the sub-micron domain into a millimeter-scale pore network resulting in a dual porosity network.
A vuggy carbonate sample was chosen and imaged at adequate resolutions (nm- to µm-scale) in order to resolve its entire pore-network system. Pore networks of the individual facies were extracted and combined according to the spatial facies distribution found in the sample. Single-phase petrophysical properties were computed and multi-phase flow simulations were run on this dual pore network and compared to the simulations performed on the single-resolution networks.

## INTRODUCTION

In the last decade, digital rock physics and pore network modeling have developed into a tool for reservoir rock characterization [1-8], which is progressively being accepted by the oil and gas industry. Continuous improvement of 3D-imaging devices now allows the construction of rock models of increasing quality at scales from around a centimeter down to nanometer (nm), - a pre-requisite to achieve accurate predictions of petrophysical properties and multi-phase flow.
While digital rock physics has been successful in homogeneous sandstones, other rock types with a range of several orders of magnitude in pore or grain sizes still pose a challenge to this technology. A model that is supposed to be representative for the rock sample must be able to resolve sub-micrometer features and at the same time capture structures that may be as large as several millimeters to centimeters. Due to hardware

limitations (computational power and image acquisition instruments), it is currently not possible to acquire and process 3D images that satisfy these requirements.
Multi-scale approaches, such as calculating petrophysical properties and multi-phase fluid flow on different images - one large-volume low-resolution and the other small-volume high-resolution - is only a partial solution. This procedure produces two distinct data sets which have to be upscaled in order to produce predictions, representative for the entire rock sample.
Numerical pore networks have been used for many years [e.g., 2; 5; 9] and offer the opportunity to combine different pore systems into one representative network. The basic approach is to acquire different 3D images with appropriate voxel resolutions to capture the sub-micron and larger scale pore network features and extract numerical pore networks from these images, correspondingly to the multi-scale approach. However, instead of calculating properties on the individual networks small-scale and large-scale networks are integrated using statistical and stochastic methods to form one pore network capturing the geometric and topologic characteristics of the largest scale imaged. This approach circumvents the above-mentioned hardware limitations because unlike grid-based data sets, the handling of numerical data sets (pore networks) does not require a large amount of computational power and is easily performed with standard personal computers. The challenge, however, is to introduce appropriate techniques for the pore network fusion in order to produce a precise-as-possible pore network model that captures the important pore system features governing single and multi-phase flow.
We present a first approach of pore network fusion using a dual porosity carbonate sample which contains a vuggy porosity and a considerable amount of micrite (sub-micron porosity). Two 3D images were acquired with different imaging tools: one larger scale at 1.2 µm voxel resolution and one small scale imaged at 65 nm voxel resolution. Numerical pore networks were extracted from both images and subsequently combined into one single pore network containing characteristics of large and small pore systems. Single-phase petrophysical properties and two-phase flow simulations were then performed on the combined network. Results are compared to simulations performed on the individual models (micro- and nano-scale).

## METHODS

The general workflow consists of five major steps:

1. Imaging and image processing: Acquisition of two (or more) 3D images with adequate volumes and voxel resolutions to resolve the different pore systems present in the rock.
2. Extraction of numerical pore networks from the individual 3D images.
3. Stochastic network generation: While the coarsest pore network remains unaltered, the high-resolution fine network is used to characterize the geometrical and topological (GT) properties in terms of probability distributions and correlations. This information is used to generate a stochastic pore network that is equivalent to the original one. Compared to the original image-derived reference network, the stochastic network is flexible in the choice of its domain and network size.

4. Network fusion: Integration of the fine stochastic pore network into the coarser pore network.
5. Simulation of petrophysical properties and two-phase flow on the combined pore network.

This work flow is described more in detail in the next sections.

**Imaging And Image Processing**

Two 3D X-ray images of a vuggy, micrite rich carbonate sample were acquired. In order to capture the vuggy porosity system, a 2 mm diameter subsample was drilled out of a core plug and was imaged at 1.2 µm voxel resolution with an Xradia MicroXCT-200 machine. An Xradia UltraXRM-L200 device was used to image a smaller subsample with a voxel resolution of 65 nm to resolve the sub-micron porosity system. Both images were cropped into cubic volumes. Prior to segmentation into pore space and solid phase the image quality was enhanced using a SUSAN filter, an edge preserving smoothing algorithm [10]. A watershed algorithm was used to segment the images into pore space and solid matter. Figure 1 gives an overview of the model dimensions, and the image processing steps.

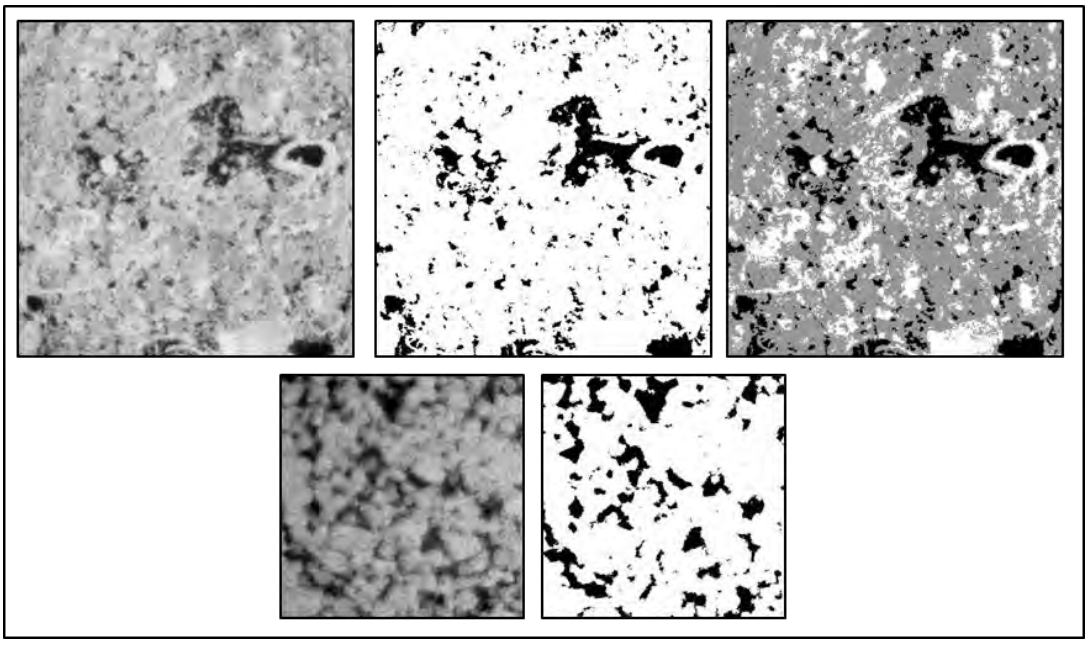

Figure 1. Upper panel: 2D slice of 3D filtered gray-scale MCT volume (left), segmented pore space (black, middle), and 3-phase segmentation into pore space (black), micrite matrix (gray), and white solid particles (right). Voxel size is 1.2 µm, image width is 1.2 mm, porosity is 10.4%. Lower panel shows 2D slice of 3D filtered gray-scale nano-CT volume (left) and the segmentation into pore space and solid to the right. Voxel size is 65 nm, image width is 30 µm and porosity amounts to 17.5%. Note that the pore structure shown in the lower panel nano-CT image represents the fine sub-micron porosity indicated in the gray color in upper right MCT image.

**Pore Network Extraction**

Numerical pore networks were extracted from both segmented volumes applying a maximal ball based network extraction [9]. With an adequate definition of discrete digital balls, the approach starts with searching all maximal balls (MB) in the pore space so that each MB touches the grain surface and is not a subset of any other MB. This procedure provides a compact representation of the pore structure with preservation of both, pore geometry and connectivity. Then, all MBs are clustered with large MBs dominating the formation of *master clusters* in which the top MBs are regarded as major parts of pores (pore-bodies) and the MBs that originate from different sub-families are pore throats. The parameters of the pore networks, such as coordination number, and pore and throat size distribution are computed directly from the chain structures formed by clusters and their connections. A detailed description of the method can be found in [9].

**Stochastic Network Generation**

Inspired by [11], a novel methodology was applied to generate a stochastic network that is equivalent to its reference network in terms of geometrical, topological and petrophysical properties [12].

The key point is to accurately obtain statistical information directly from the reference network and its underlying image. A suite of methods is used to calculate the probability distributions for radius, volume, length etc., and the correlations between pores and throats, as well as the connectivity function for the entire pore network [12]. In addition to these characteristics, a spatial function between network elements is introduced, which is similar to the concept of a two-point correlation function, in order to describe the heterogeneity of complex pore structures.

The next step is to create a defined number of pores and throats with exactly the same geometrical properties as the reference network and a proper connection between pores and throats under the following conditions:

- Matched coordination number distribution (large pores tend to have a higher coordination number;
- Appropriate correlations between pores and throats (aspect ratio);
- Connection probability: the smaller the distance between two pores, the larger is the probability of being connected, but under the control of a pore distance distribution with a restriction on the maximal distance [13, 14].

Figure 2 illustrates the equivalence of the generated stochastic network and the original fine nano-CT derived pore network with respect to the pore/throat radius distribution, connectivity function and shape factor.

**Network Fusion**

Once the stochastic network equivalent matches the original fine pore network satisfactory, the coarse (MCT-derived) pore network and the fine, stochastic (nano-CT equivalent) networks are combined to build one pore network containing dual porosity systems. In pore-network fusion, three main issues have to be addressed very carefully: (1) to preserve the spatial distribution of networks with respect to their sizes and

domains, (2) to define the cross-connection between networks, and (3) to choose network elements to be retained or to be discarded.

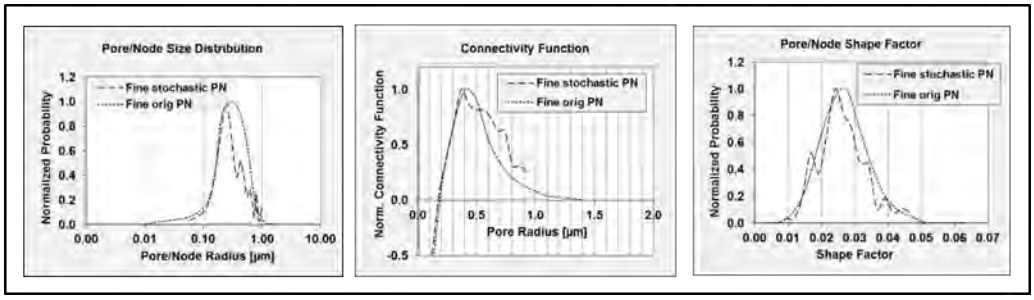


Figure 2. Comparison of original nano-scale pore network and calculated stochastic network equivalent with respect to pore and node sizes distributions (left), connectivity function (middle) and shape factors (right). Size distributions and shape factors are calculated on the entire pore network (pores and pore throats).

(1) The first issue is mainly related to preservation of the heterogeneous nature of the rock sample, predominantly mirrored in the coarse network, which contains the larger structures (e.g. vuggy porosity). The fine (nano-CT derived) pore network contains only nm-scale pores and is considered as more homogeneous compared to the large, vuggy one. In order to preserve the critical structure and heterogeneity of the sample during the fusion process, the dual pore network is generated directly based on the MCT-image derived coarse network itself, rather than creating a stochastic network for this one as well. This unaltered coarse network determines the physical network domain. Sub-micron scale network elements are then added into this domain.
(2) The second issue is to determine how to create cross connections between the coarse and fine networks. Based on the rock structure it is unreasonable to connect a fine nano pore to a coarse, vuggy micro pore with a coarse, micron-sized throat. In the case of micrite rich, vuggy carbonates there are only two main possibilities: either the vuggy porosity is connected by itself then this pore system has own micro-scale throats; or the vuggy porosity is only connected through the micrite matrix, which is nano-scale. (Of course there is the option that the vugs are not connected at all, but this is not relevant here because in this case the vugs will not contribute to flow.) Therefore, we consider the cross-connection between fine pores and coarse pores by fine throats, only.
(3) The last issue is to determine which pores and throats are kept in the resulting dual pore network to avoid spatial overlap between the two networks. In order to achieve this, first the fine stochastic network must be generated in the same physical space (not the lattice represented by a cube of voxels) of the original coarse pore network and second the overlapping structures are eliminated according to the following rules: (1) Fine pores /throats that are completely covered by coarse network elements are to be discarded (note that generally no overlap should occur and a better way of the spatial correlation of the pore networks will be implemented); (2) each fine throat that cross the boundary between a coarse pore and a fine pore is retained; and (3) all other coarse and fine network elements are retained. Figure 3 illustrates the described rules along with the fine

stochastic nano pore network, the original coarse network and the combined dual porosity pore network.

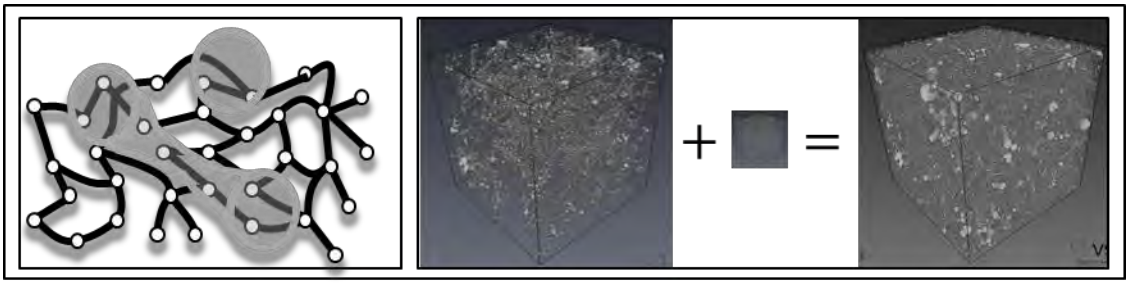

Figure 3. Left: Rules for elimination of overlapping structures as described in text: lower gray-shaded area (coarse network elements) shows fine pores and throats completely covered by coarse elements that will be eliminated (1), upper gray shaded circle shows case (2), where fine throats are retained because they cross the boundary between coarse and fine pores. Right: illustrations of pore network fusion of coarse network + fine network = combined network.

**Flow simulations**

Flow simulations are performed on the combined pore network running a two-phase code developed by [5]. All simulations are run for a water/oil system, oil density is 800 kg/m$^3$, water density is 1050 kg/m$^3$, with an interfacial tension between oil and water of 27 mN/m. Initially fully water filled, carbonate rocks, which are oil charged are known to change their wettability towards oil wet or mixed wet conditions. The wettability preference is not only a factor of mineralogy but also sensitive to facies distribution and many other partially still unknown factors. Since the reservoir the sample was derived is known to be oil wet, 70% of the pore volumes were randomly assigned oil wet conditions. All flow simulations were run with the same setup to assure that all differences in results are due to the intrinsic properties of the rock and not caused by altered input parameters. The fitting of the capillary pressure curves and the relative permeability curves was performed according to [15] and [16], respectively.

## RESULTS AND DISCUSSION

The studied carbonate rock is made up by 37% solid calcite (bioclasts and cemented area), 52% microcrystalline (micrite) matrix, and 10.4% vuggy porosity (biomolds, intraparticle porosity and solution enlarged biomolds and intraparticle porosity; see Fig. 1, right upper panel). Thus, the sample contains a dual porosity system, a coarse pore system with vugs up to larger than hundred μm across and a micritic nano porosity. The coarse-scale vuggy porosity system captured with the MCT image covers a volume with 1.2 mm side length, that of the (nano-CT derived) micrite porosity a volume with 30 μm side length. Figure 1 indicates that there is additional nano porosity below the resolution of the scan which cannot be resolved (or was discarded during image processing). However, we assume that this represents only a small fraction of the total porosity and does not significantly affect our results.

The goal of this study is to combine micro-scale and nano-scale information into one pore network and extract petrophysical properties and two-phase flow parameters from this fused pore network. Taking the full size of the coarse network as physical domain and fusing this with the nano-scale network would result in > 200 million network elements in the combined pore network. Although this would be the preferred choice to capture the maximum heterogeneity it is currently not possible to perform flow simulations on such a pore network. In order to keep the network elements in a manageable size, one third (36%) of the coarse network was chosen as physical domain. The combined network has a physical size of 480 $\mu m^3$ and contains approx. 425,000 network elements (pores and pore throats). This size of 480 $\mu m^3$ resolved down to 65 nm would correspond to an image with 7385 voxels side length and 403 billion grid cells.

Flow simulations were performed on the original MCT-derived pore network (coarse network), on the original fine nano-CT-derived (not the stochastic equivalent), and on the combined pore network using the same input parameters and assigning 70% oil-wet pores. The choice of the wettability preference is a very important factor and is not straightforward. Several contradictory theories can be found in literature. In absence of exact knowledge of the wettability distribution the oil wet regions were distributed evenly between vuggy pores and micrite pores. The flow simulations were run under oil wet conditions because the sample originates from a reservoir that is known to be oil wet.

Table 1 gives an overview about the rock model parameter, the extracted petrophysical properties, pore-network statistics and end point saturations of two-phase flow simulations. Figures 4 through 6 show the results of the flow simulations performed on the coarse (MCT-derived) pore network, the fine (nano-CT derived) network and the combined network, respectively.

Table 1. Rock model parameter, single phase petrophysical properties, pore-network statistics and end state saturations of multi-phase flow simulations. PN: pore network, Swi: residual water saturation, Sor: residual oil saturation, krw@Sor: water relative permeability at residual oil saturation.

| Property: | Coarse MCT | Fine nano-CT | Combined |
|---|---|---|---|
| Model Size (vx) | $1000^3$ | $450^3$ | -- |
| Voxel Size (µm) | 1.17 | 0.065 | -- |
| Model Size (µm) | $1170^3$ | $29.25^3$ | $480^3$ |
| Image Porosity | 0.104 | 0.175 | -- |
| Volume micrite | 0.52 | This is the micrite | -- |
| PN Porosity | 0.098 | 0.147 | 0.195 |
| PN Permeability (mD) | 0.7 | 0.28 | 1.2 |
| PN Formation Factor | 2524 | 72 | 21 |
| Cementation exponent | 3.46 | 2.2 | 1.86 |
| No. of Pores | 34485 | 1124 | 188410 |
| No. of Pore throats | 45033 | 1356 | 237270 |
| Swi | 0.44 | 0.09 | 0.02 |
| Pc crossover Sw | 0.5 | 0.15 | 0.11 |
| Sor | 0.47 | 0.12 | 0.18 |
| krw@Sor | 0.00 | 0.89 | 0.87 |

The coarse MCT-derived pore network shows a porosity of 10.4% and an absolute permeability of 0.7 mD (Table 1). The low absolute permeability indicates that this sample does not have a well-connected vug system, which typically would have two to three orders higher permeability. This finding is corroborated by the very high formation factor. Calculation of the percolating porosity shows that only approximately half of the porosity (5.1%) is connected in two directions, while the model is not percolating in the third direction. The voxel resolution of 1.2 µm is just sufficient to resolve a few of the largest throats that connect some of the vugs in the pore system. Moreover, the similarity of the permeability to the permeability of the fine nano-CT derived network (0.7 versus 0.28 mD) suggests that these pore throats are actually the same as the larger connections in the nm-resolved network. The flow simulations show that there is hardly any two-phase flow in the coarse pore network (Fig. 4). The pore system imaged at this coarse resolution can only be used to retain the vuggy characteristics for the pore network fusion.

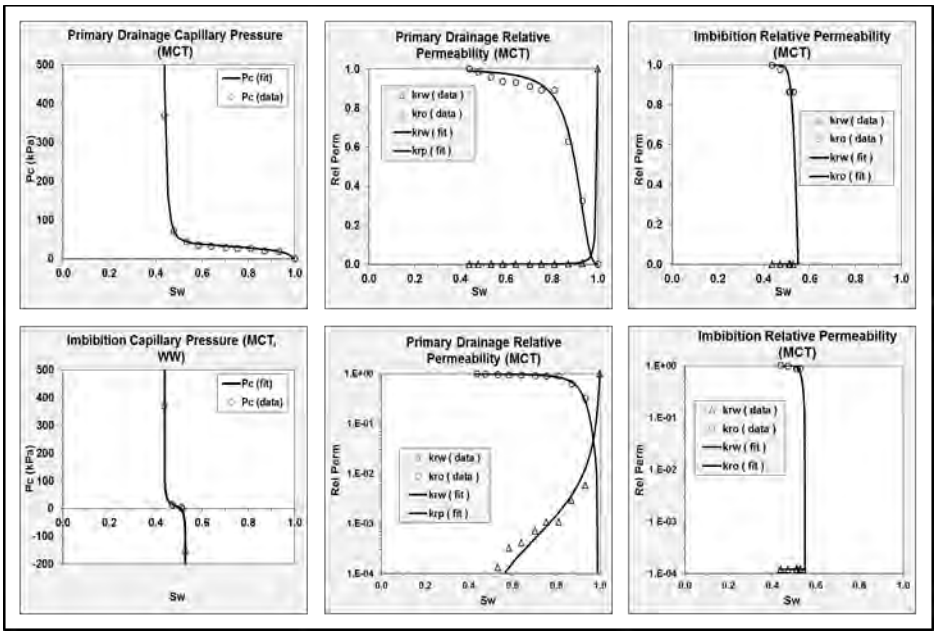


Figure 4. Two phase fluid flow simulation capillary pressure curves (left) and relative permeability curves (middle and right column) of coarse MCT-derived network.

The high-resolution nano-CT derived pore network has regular properties of a micrite facies. For the given porosity of 17.5% the permeability (0.28 mD) and the formation factor (72) are in the typical range for this rock type (Table 1). Also the results of the two-phase flow simulations, with an initial water saturation of 9% and a residual oil saturation of 12% are representative for an oil-wet microcrystalline carbonate rock (Table 1; Fig. 5). With only approx. 2,500 network elements this network is on the lower limit for a pore network to produce sophisticated multi-phase flow results. Consequently, the relative permeability curves show finite size effects, such as a jump of oil connectivity at 70% water saturation during drainage and a late connection of the water phase (at 53%

Sw) during imbibition (Fig. 5). Nevertheless, the simulated results are believed to be reliable since micrite facies is fairly homogeneous and simulated permeability and formation factor match published values for this rock type.

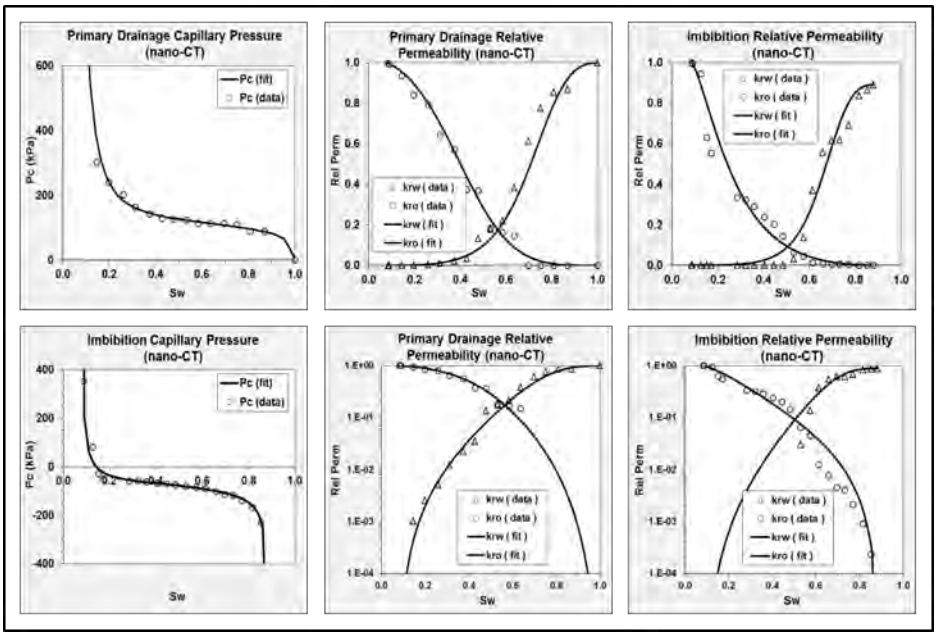


Figure 5. Two phase fluid flow simulation capillary pressure curves (left) and relative permeability curves (middle and right column) of fine nano-CT-derived network.

The combined network has a porosity of 19.5% and the absolute permeability of 1.2 mD is, as expected, higher than the ones calculated on the coarse MCT and the fine nano-CT derived networks. This is expected, since the mean hydraulic radius for flow was already captured in both networks (even if the coarse one was hardly connected). Through fusion of the two networks, (formerly missing) connectivity is added, reducing the tortuosity and thus, increasing the permeability. The same pore network fusion that only slightly increased the permeability lowered the formation factor to 20 versus >2500 in the badly connected coarse network and 72 in the nano-network. This reduces the calculated cementation exponent to 1.86 in turn of 2.2 calculated for the micrite nano-network alone, (and 3.5 for the coarse non-connected vuggy pore system). This might have severe implications for reservoir rock quality characterization and estimation of fluid saturations. Figure 6 displays the results of the two-phase flow simulation performed on the combined network. The results suggest a “well behaved” rock in terms of capillary pressure curves and relative permeability for the primary drainage and the imbibition process i.e., the curves and the end point saturations are in good accordance with observations made on similar carbonate rocks. Some plateaus are visible in the oil relative permeability curve during drainage and the water relative permeability curve during imbibition. The cause of these plateaus is currently not known. However, as stated above the fine nano network has too few pores and throats and shows finite size effects in

the relative permeability curves. It would be only logical if these finite size artifacts would translate themselves into the combined pore network.

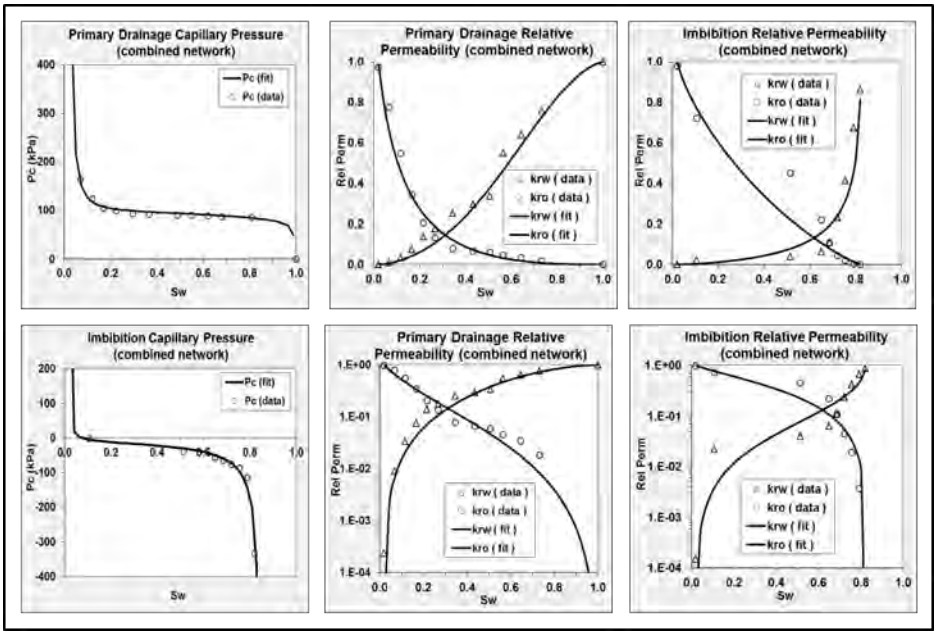


Figure 6. Two phase fluid flow simulation capillary pressure curves (left) and relative permeability curves (middle and right column) of combined network.

Figure 7 gives a comparison of the capillary pressures and relative permeability curves extracted from the coarse, the fine and the combined pore networks. It is evident that the coarse network cannot produce reliable results – the resolution of the MCT image it is derived from is simply not good enough. By chance, the voxel resolution of 1.2 µm is just sufficient to produce a reasonable absolute permeability but it fails to capture the characteristics responsible for the electric properties and for two-phase flow.

Next to the finite size effects, the nano-CT network produces good results in terms of petrophysical properties and two-phase flow. Initial water saturation and residual oil saturation are expected values for an oil-wet micrite – however, end point saturations and relative permeability curves are only representative for the micrite facies and do not mirror the effects of the additional vuggy pore system. The importance of capturing the dual porosity system is most evident in the capillary pressure curves (Fig. 7). While the drainage entry pressure is the same for the micrite pore system and the combined dual porosity system, the micritic nano network fails to predict the capillary pressure properties of the rock over the full range of water saturations. Moreover, initial water saturation and residual oil saturation are lower and the cross-over point is at lower water saturation for the combined dual porosity network compared to the micrite nano network (Table 1, Fig. 7).

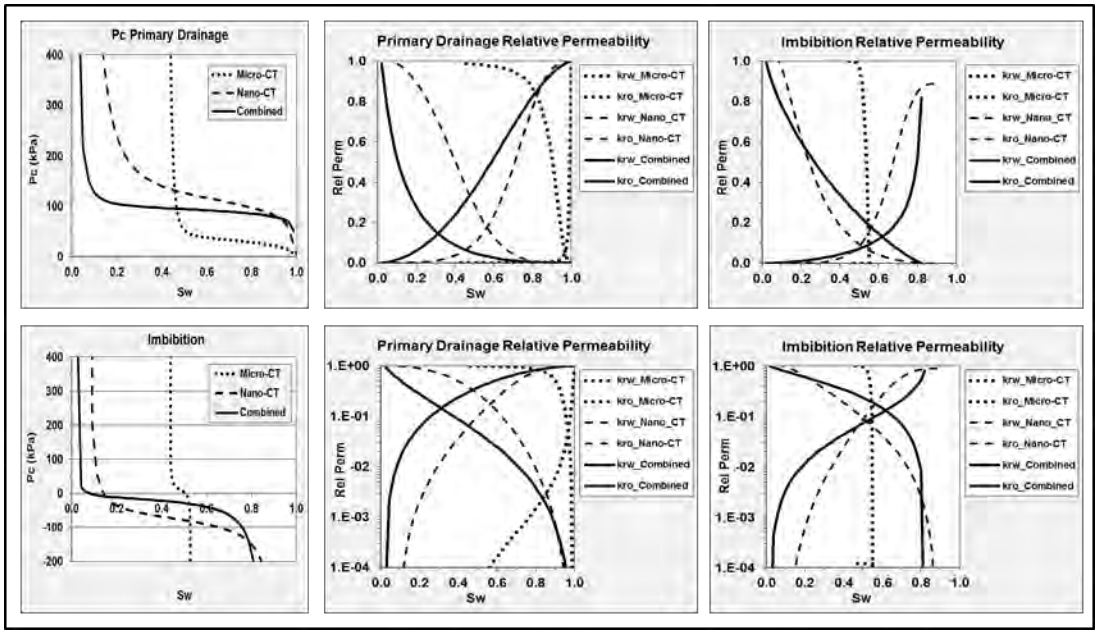


Figure 7. Comparison of two phase fluid flow simulation capillary pressure curves (left) and relative permeability curves (middle and right column) between coarse, fine, and combined network.

## CONCLUSIONS

A novel technique is presented that is capable to combine pore networks derived from X-ray images that were acquired with 20-fold difference in voxel resolution (1.2 µm versus 65 nm) and have 40 times difference in physical size (1.2 mm versus 30 µm). The combined pore network contains information on pore systems, which cover approximately four orders of magnitude in size (from 150 nm to larger than 100 µm). Extracted petrophysical properties are commensurate to comparable rock types and the simulated two-phase flow properties highlight the importance of capturing the full characteristics of the rock in order to achieve meaningful results.

Parallelization of the two-phase flow simulation code is needed to run simulations on the full physical domain size of the coarse network (instead on a reduced domain) to capture the maximum heterogeneity of the rock as present in the coarse network.

Several finite-size artifacts observed in the relative permeability curves indicate that the combined pore network is not perfect leaving space for future improvement, while it is not known if these effects were caused by the shortcoming of the original fine network or by the network fusion process itself.

## ACKNOWLEDGEMENTS

We thank Shehadeh K. Masalmeh and Xu-Dong Jing from Shell Global Solutions International for providing the studied sample and for the allowance to publish results.

## REFERENCES

[1] Blunt, M.J., Jackson, M.D., Piri, M. and Valvatne, P.H., "Detailed physics, predictive capabilities and macroscopic consequences for pore-network models of multiphase flow", *Advances in Water Resources*, (2002), **25**, 1069-1089

[2] Bakke, S., Øren P-E., "3-D pore-scale modelling of sandstones and flow simulations in the pore networks", *SPE J.*, (1997), **2**, 136-49.

[3] Øren, P-E., Bakke, S., "Process based reconstruction of sandstones and prediction of transport properties", *Transport Porous Med.*, (2002), **46**, 2-3, 311-43.

[4] Patzek, T.W., "Verification of a complete pore network simulator of drainage and Imbibition", *SPE J.*, (2001), **6,** 144-56.

[5] Valvatne, P.H., Blunt, M.J., "Predictive pore-scale modeling of two-phase flow in mixed wet media", *Water Resources Research,* (2004), **40**, W07406, http://dx.doi.org/10.1029/2003WR002627.

[6] Piri, M., Blunt, M.J., "Three-dimensional mixed-wet random pore-scale network modeling of two- and three-phase flow in porous media. I. Model description", *Phys Rev E,* (2005), **71**, 026301.

[7] Piri, M., Blunt, M.J., "Three-dimensional mixed-wet random pore-scale network modeling of two- and three-phase flow in porous media. II. Results", *Phys Rev E,* (2005), **71**, 026302.

[8] Arns, J.Y., Sheppard, A.P., Arns, C.H., Knackstedt, M.A., Yelkhovsky, A., Pinczewski, W.V., "Pore-level validation of representative pore networks obtained from micro-CT images", *In: Proceedings of the Annual Symposium of the Society of Core Analysis*, SCA2007-A26, 2007, Calgary, Canada.

[9] Dong, H., Blunt, M., "Pore-network extraction from micro-computed tomography images", *Phys. Rev. E*, (2009) **80**, 036307.

[10] Smith, S.M., Brady, J.M., "SUSAN-Anew Approach fo Low Level Image Processing", *International Journal of Computer vision*, (1997), **23**, 1, 45-78.

[11] Idowu, N.A., Blunt, M.J., "Pore-Scale Modeling of Rate Effects in Waterflooding", *Transort in Porous Media*, (2010), **83**, 151-169.

[12] Jiang, Z., van Dijke, M.I.J., Wu, K., Couples, G.D., Sorbie, K.S., Ma, J., "Stochastic Pore Network Generation from 3D Rock Images", *Transp. Porous. Med.*, (2011), DOI 10.1007/s11242-011-9792-z.

[13] Vogel, H.J., "Morphological determination of pore connectivity as a function of pore size using serial sections", *European Journal of Soil Science*, (1997), **48**, 365–377.

[14] Vogel, H.J., Roth, K., "Quantitative morphology and network representation of soil pore structure", *Advance in Water Research Resource*, (2001), **24**, 233-242.

[15] Skjæveland, S.M., Siqveland, L.M., Kjosavik, A., Hammervold Thomas, W.L., and Virnovsky, G.A., "Capillary Pressure Correlation for Mixed-Wet Reservoirs", *SPE Reservoir Evaluation & Engineering*, 2000, **3** (1), 60-67.

[16] Lomeland, F., Ebeltoft, E., and Thomas, W. H., "A new versatile relative permeability correlation", *In: Proceedings of the Annual Symposium of the Society of Core Analysis,* SCA2005-032, 2005, Toronto, Canada.